Differentiation of V2a interneurons from human pluripotent stem cells

Jessica C. Butts[a,b], Dylan A. McCreedy[a,c,d], Jorge Alexis Martinez-Vargas[e], Frederico N. Mendoza-Camacho[a], Tracy A. Hookway[a], Casey A. Gifford[a], Praveen Taneja[f], Linda Noble-Haeusslein[c,d], and Todd C. McDevitt[a,g,1]

[a]Gladstone Institute of Cardiovascular Disease, San Francisco, CA 94158; [b]Graduate Program in Bioengineering, University of California, San Francisco, CA 94158; [c]Department of Neurosurgery, University of California, San Francisco, CA 94143; [d]Department of Physical Therapy and Rehabilitation Science, University of California, San Francisco, CA 94143; [e]Department of Bioengineering, University of California, Berkeley, CA 94709; [f]Gladstone Institute of Neurological Disease, San Francisco, CA 94158; and [g]Department of Bioengineering and Therapeutic Sciences, University of California, San Francisco, CA 94158

Edited by Tom Maniatis, Columbia University Medical Center, New York, NY, and approved March 29, 2017 (received for review June 13, 2016)

The spinal cord consists of multiple neuronal cell types that are critical to motor control and arise from distinct progenitor domains in the developing neural tube. Excitatory V2a interneurons in particular are an integral component of central pattern generators that control respiration and locomotion; however, the lack of a robust source of human V2a interneurons limits the ability to molecularly profile these cells and examine their therapeutic potential to treat spinal cord injury (SCI). Here, we report the directed differentiation of CHX10$^+$ V2a interneurons from human pluripotent stem cells (hPSCs). Signaling pathways (retinoic acid, sonic hedgehog, and Notch) that pattern the neural tube were sequentially perturbed to identify an optimized combination of small molecules that yielded ∼25% CHX10$^+$ cells in four hPSC lines. Differentiated cultures expressed much higher levels of V2a phenotypic markers (CHX10 and SOX14) than other neural lineage markers. Over time, CHX10$^+$ cells expressed neuronal markers [neurofilament, NeuN, and vesicular glutamate transporter 2 (VGlut2)], and cultures exhibited increased action potential frequency. Single-cell RNAseq analysis confirmed CHX10$^+$ cells within the differentiated population, which consisted primarily of neurons with some glial and neural progenitor cells. At 2 wk after transplantation into the spinal cord of mice, hPSC-derived V2a cultures survived at the site of injection, coexpressed NeuN and VGlut2, extended neurites >5 mm, and formed putative synapses with host neurons. These results provide a description of V2a interneurons differentiated from hPSCs that may be used to model central nervous system development and serve as a potential cell therapy for SCI.

V2a interneurons | human pluripotent stem cells | differentiation | single-cell RNAseq

Cell replacement is a promising therapeutic strategy to restore motor function and sensation after traumatic injury to the central nervous system (CNS). Several clinical trials are currently investigating the therapeutic efficacy of various transplanted neural cells to treat spinal cord injury (SCI), including oligodendrocyte progenitors derived from human embryonic stem cells (hESCs) (1), autologous Schwann cells (2), and fetal-derived neural stem cells (3) and precursor cells (4, 5). Despite such efforts, however, the ability of specific neuronal cell types to functionally restore damaged neural networks needs further investigation.

Pluripotent stem cells (PSCs) provide a renewable source of cells that can differentiate into a variety of neurons, provided that the necessary signaling cues are presented in an appropriate spatiotemporal manner. Different types of neurons, including forebrain and midbrain neural cell types, such as cortical neurons (6), dopaminergic neurons (7), and inhibitory interneurons from the medial ganglionic eminence (8, 9), have been differentiated from hPSCs, but motor neurons are the only caudal neuronal population to be generated from hPSCs to date (10, 11).

V2a spinal interneurons in particular are crucial to the transmission and coordination of motor and sensory functions (12, 13). Glutamatergic V2a interneurons, identified by expression of the CHX10 transcription factor (14), are distributed throughout the hindbrain and spinal cord in mammals and relay excitatory stimuli to central pattern generators that regulate motor function for breathing and locomotion (15–19). Ablation of V2a interneurons in mice results in disruption of normal breathing patterns (18), impaired forelimb reaching tasks (15), and loss of left-right hindlimb coordination (16, 17).

Combinations of various morphogenic signals are responsible for patterning of the neural tube during development. The rostral-caudal location of spinal cell types is patterned by retinoic acid (RA) released from adjacent somites (20). In parallel, an orthogonal ventral-dorsal gradient of sonic hedgehog (Shh), secreted from the floor plate and notochord, specifies independent progenitor domains (21) that yield mature cell types with distinct roles in motor function. In the ventral neural tube, excitatory V2a and inhibitory V2b interneurons arise coincidentally from the p2 domain (22, 23), which is located immediately dorsal to the pMN domain. Notch signaling dictates the balance between V2a and V2b interneurons, with Notch signaling necessary for the specification of V2b interneurons and Notch inhibition increasing the proportion of V2a interneurons (Fig. 1*A*) (24).

This study provides a description of human V2a interneurons differentiated from PSCs with small molecule agonists and antagonists of developmental signaling pathways. We investigated

Significance

Spinal cord injury (SCI) significantly disrupts normal neural circuitry, leading to severe degradation of motor and sensory function. Excitatory interneurons that relay signals from the brain to neural networks throughout the spinal cord, including glutamatergic V2a interneurons that coordinate respiration and locomotion, are lost after SCI. Thus, transplantation of V2a interneurons after SCI could provide a novel therapy to restore functional connections between the brain and spared downstream neurons. This study describes the generation of V2a interneurons from human pluripotent stem cells, using developmentally relevant morphogenic signaling pathways. This work provides initial insight into the development of excitatory human interneurons and enables the examination of their therapeutic efficacy for SCI repair.

Author contributions: J.C.B., D.A.M., J.A.M.-V., T.A.H., C.A.G., P.T., L.N.-H., and T.C.M. designed research; J.C.B., D.A.M., J.A.M.-V., F.N.M.-C., C.A.G., and P.T. performed research; C.A.G. contributed new reagents/analytic tools; J.C.B., D.A.M., T.A.H., C.A.G., P.T., L.N.-H., and T.C.M. analyzed data; and J.C.B., D.A.M., J.A.M.-V., T.A.H., C.A.G., P.T., L.N.-H., and T.C.M. wrote the paper.

The authors declare no conflict of interest.

This article is a PNAS Direct Submission.

Data deposition: The sequencing data have been deposited in the National Center for Biotechnology Information's Sequence Read Archive (accession no. GSE97564).

[1]To whom correspondence should be addressed. Email: todd.mcdevitt@gladstone.ucsf.edu.

This article contains supporting information online at www.pnas.org/lookup/suppl/doi:10.1073/pnas.1608254114/-/DCSupplemental.

the specificity of the defined protocol and the ability of the differentiated cells to mature into excitatory neurons in vitro and in vivo. These results provide a robust source of human V2a interneurons that can be used to further define their molecular profile and in vitro electrophysiological properties, as well as to examine their therapeutic potential for repair of spinal cord injury.

Results

hPSC-Derived V2a Interneuron Differentiation Depends on RA, Shh, and Inhibition of Notch Signaling. Motor neurons, which arise ventral to V2a interneurons, have been differentiated from hPSCs in ~3 wk with dual SMAD inhibition, followed by RA and Shh agonists (11). Thus, using a similar time course, the concentrations of known morphogens and signaling pathways that specify V2a commitment [RA, Shh, and the Notch inhibitor *N*-[(3,5-difluorophenyl)acetyl]-L-alanyl-2-phenyl]glycine-1,1-dimethylethyl ester (DAPT)] in mouse embryonic stem cells (ESCs) (25, 26) were sequentially varied independently, and the percentages of $CHX10^+$ cells differentiated from hPSCs at day 17 were examined. An RA concentration of 100 nM starting at day 5 of culture with fixed concentrations of the Shh agonist purmorphamine (pur; 1 μM) and DAPT (5 μM) (both beginning on day 7) resulted in the greatest $CHX10^+$ population at day 17 (~6%; Fig. 1*C*). Following that, treatment with 100 nM pur beginning at day 7 with 100 nM RA and 5 μM DAPT resulted in ~30% $CHX10^+$ cells after 17 d of differentiation (Fig. 1*D*). Finally, the concentration of DAPT was varied beginning on day 7 with fixed RA and pur concentrations (100 nM each), and 1 μM and 5 μM DAPT resulted in comparable $CHX10^+$ populations (~20%; Fig. 1*E*). Regardless of morphogen concentration, $CHX10^+$ cells appeared to be evenly distributed throughout the differentiating cultures (Fig. 1 *F*–*H*).

Because DAPT concentrations of 1 μM and 5 μM yielded similar efficiencies of V2a interneuron differentiation, we examined the effects of these concentrations on the efficiency of $CHX10^+$ differentiation. Given that higher concentrations of small molecule inhibitors, such as DAPT, are often more cytotoxic (27), we examined the total number of cells and yield of $CHX10^+$ cells per input number of PSCs. A lower DAPT concentration (1 μM) yielded more viable cells than cultures treated with 5 μM DAPT (4.40 million cells vs. 2.85 million cells per well of a 24-well plate; *SI Appendix*, Fig. S1*B*), resulting in a ~50% increase in the number of $CHX10^+$ cells per input PSC (*SI Appendix*, Fig. S1*C*). Varying the onset of Notch inhibition by initiating DAPT treatment on day 5, 7, or 10 of differentiation (*SI Appendix*, Fig. S1*D*) yielded similar percentages of $CHX10^+$ cells; thus, DAPT was added at day 7 for all subsequent studies to coincide with the introduction of pur. In addition, a seeding density of 25,000 cells per cm^2 resulted in a greater percentage of $CHX10^+$ cells compared with a density of 5,000 or 100,000 cells per cm^2 (*SI Appendix*, Fig. S1*E*). Overall, these results demonstrate the ability of hPSCs to robustly differentiate into putative V2a interneurons by RA and Shh agonists in combination with Notch inhibition.

Differentiation of V2a Interneurons from hPSCs Is Specifically Enriched. We analyzed gene expression throughout the first 17 d of differentiation to characterize the temporal changes in the V2a interneuron cell population (Fig. 2*A*). As expected, expression of the pluripotency gene *POU5F1* (all gene descriptions in *SI Appendix*, Table S2) decreased by day 3 and remained significantly down-regulated through day 17. Early markers expressed during neural tube development (*PAX6* and *NES*) increased by day 7. Other markers of spinal cell types expressed in the ventral neural tube (*GATA3*, *OLIG2*, *HB9*, and *SIM1*) were detected as early as day 3 and continued to increase throughout differentiation. Expression of markers for the p2 domain (*FOXN4*) and committed V2a interneurons (*CHX10* and *SOX14*) began on day 10 and were highly up-regulated by day 15. Expression of neuronal genes (*TUBB3* and *NEFL*) was significantly up-regulated (~10- and ~70-fold, respectively) at day 17, whereas expression of glial (*PDGFRA*, *CSPG4*, *SOX10*, and *GFAP*) and retinal (*THY1*, *IRBP,* and *CRX*) genes was not (Fig. 2*B*). Taken together, these results demonstrate

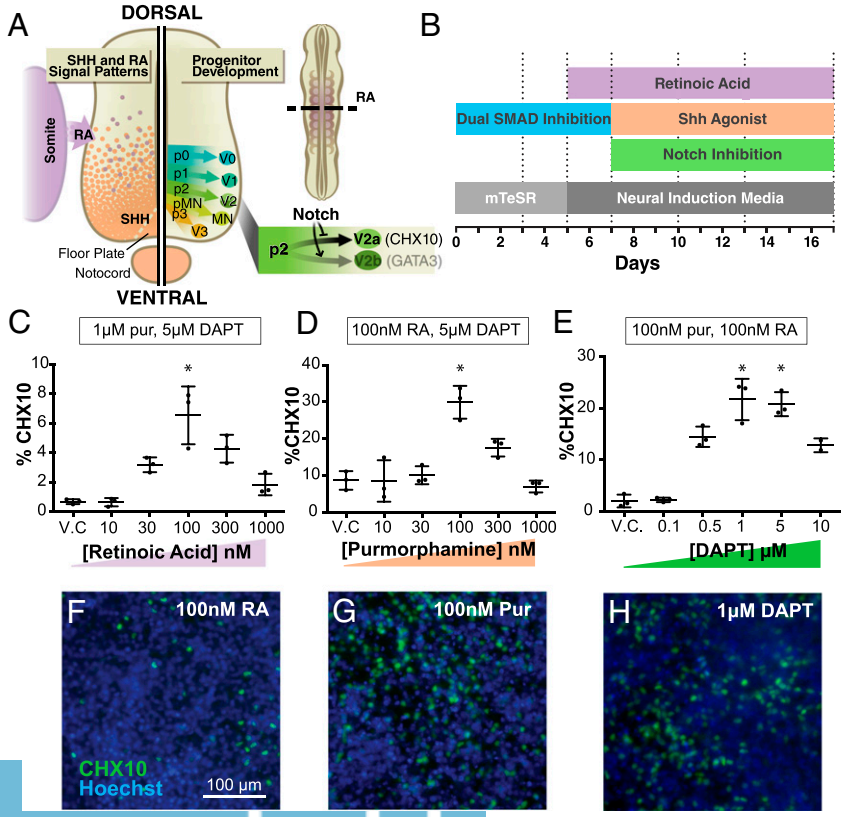

Fig. 1. Morphogen concentrations modulate V2a interneuron population. (*A*) Schematic of the developing neural tube. RA, released from the somites, and Shh, released from the floorplate and notochord, pattern the different progenitor domains of the neural tube. Notch signaling is necessary for generating V2b interneurons, whereas Notch inhibition promotes V2a interneuron differentiation. (*B*) Timeline of the V2a interneuron protocol. (*C*) Flow cytometry analysis of CHX10 expression as RA concentration was varied, and Shh agonist pur and DAPT concentrations were held constant. CHX10 expression using 100 nM RA was greater ($P < 0.05$, one-way ANOVA and Tukey's post hoc comparison) than that in the vehicle control (V.C., DMSO), 10 nM, 30 nM, and 1 μM groups. (*D*) Flow cytometry analysis of CHX10 expression as pur concentration was varied and RA and DAPT concentrations were held constant. CHX10 expression using 100 nM pur was greater ($P < 0.05$, one-way ANOVA and Tukey's post hoc comparison) than that of all groups. (*E*) Flow cytometry of CHX10 expression as DAPT concentration was varied, and RA and pur concentrations were held constant. CHX10 expression using 1 μM and 5 μM DAPT was greater ($P < 0.05$, one-way ANOVA and Tukey's post hoc comparison) than that in the V.C, 100 nM, and 500 nM groups. (*F*–*H*) Immunostaining for CHX10 (green) and nuclei labeling (blue) of differentiations with 100 nM RA (*F*), 100 nM pur (*G*), or 1 μM DAPT (*H*). $n = 3$. Data represent mean ± SD. (Scale bar: 100 μm.)

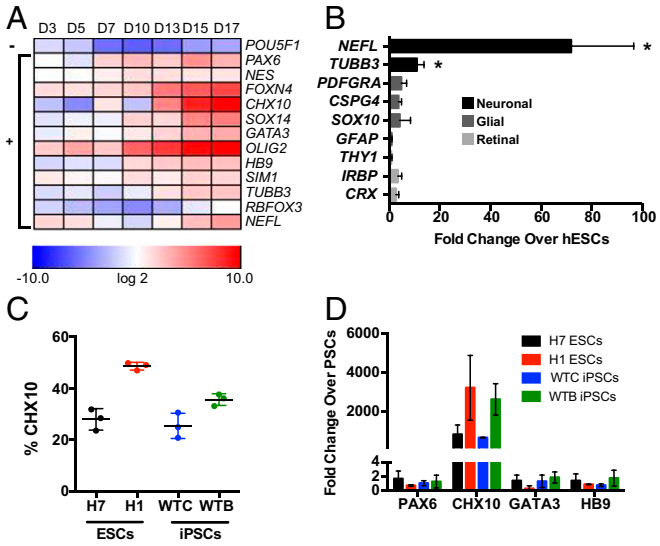

Fig. 2. V2a interneuron protocol robustly increases hPSC neurogenesis. (*A*) Gene expression throughout V2a interneuron differentiation compared with undifferentiated H7 hESCs. − indicates that gene expression is significantly down-regulated (slope coefficient negative and different from 0, $P < 0.05$ using a linear time-trend model) through culture duration. + indicates that gene expression is significantly up-regulated (slope coefficient positive and different from 0; $P < 0.05$ using a linear time-trend model) throughout the duration of culture. (*B*) Neuronal, glial, and retinal gene expression at day 17 compared with H7 hESCs. NEFL and TUBB3 expression was increased by more than twofold ($P < 0.05$, unpaired *t* test). (*C*) CHX10 percentage of ESCs (H7 and H1) and iPSCs (WTB and WTC) differentiated with the V2a interneuron protocol. (*D*) Gene expression at day 17 compared with PSCs. Data represent mean ± SD.

that the observed gene expression profile of the population is consistent with the expected phenotype of V2a interneurons.

To determine the reproducibility of V2a interneuron differentiation, we tested the resulting protocol (i.e., 100 nM RA, 100 nM pur, and 1 μM DAPT) on several additional hPSC lines (H1 ESCs, WTC iPSCs, and WTB iPSCs). We obtained robust CHX10$^+$ populations in all of the lines examined, with efficiencies ranging from ∼25% to 50% (Fig. 2*C*). Expression of spinal neuronal markers was examined at day 17 for each of the hPSC cell lines, and *CHX10* levels were consistently high, whereas markers for early neural tube development (*PAX6*) and other neuronal subtypes (*HB9* and *GATA3*) were low (Fig. 2*D*). No discernible spatial patterns were observed for CHX10$^+$ cells in any of the differentiating cultures (*SI Appendix*, Fig. S2*A*). Over the course of more than a dozen independent differentiation studies, CHX10$^+$ percentages >20% were routinely achieved (*SI Appendix*, Fig. S2*B*). These data demonstrate the establishment of a robust neuronal differentiation process that reproducibly yields enriched cultures of V2a interneurons from hPSCs.

The specificity of the V2a interneuron protocol was examined by direct comparison with a common human motor neuron protocol (11) (Fig. 3*A*). After 17 d of differentiation, the V2a interneuron differentiation yielded ∼30% CHX10$^+$ cells, whereas the motor neuron differentiation yielded very few CHX10$^+$ cells (<1%; Fig. 3*B*). CHX10$^+$ nuclei and β_{III} tubulin expression were more abundant under the V2a interneuron differentiation protocol compared with the motor neuron conditions (Fig. 3*C*, *i* and *ii*). In addition, more OLIG2$^+$ (progenitor motor neuron marker) nuclei were yielded by the motor neuron differentiation conditions than by the V2a interneuron protocol (Fig. 3*C*, *iii* and *iv*). Although the expression of neuronal genes (*NEFL*, *TUBB3*, and *PAX6*) was slightly elevated with the V2a interneuron differentiation, the V2a interneuron transcription factors (*CHX10* and *SOX14*) exhibited the greatest increase in expression (∼100-fold) relative to motor neuron cultures. Expression of other lineage markers (*GATA3*, *FOXN4*, *OLIG2*, and *HB9*) did not appear to differ between the two differentiation processes, however (Fig. 3*D*). Collectively, these results demonstrate that the V2a differentiation conditions specifically enrich for CHX10$^+$ interneurons.

We performed single-cell RNAseq analysis to define the cellular composition of the heterogeneous cultures. Seven distinct clusters of cells (designated A–G) were identified by *k*-means clustering using 12 principal components (Fig. 4*A*) with 77% of *CHX10*$^+$ cells contained within cluster B (Fig. 4*B*). The top globally differentially expressed genes were used to distinguish the general phenotypes of the seven clusters that defined the total population (Fig. 4*C* and *SI Appendix*, Table S1). Gene ontology (GO) analysis and individual inspection of the top differentially expressed genes (*SI Appendix*, Figs. S3–S5) suggested that clusters A and B were committed neurons [neuralfilament medium polypeptide (*NEFM*) and *NSG1*], cluster C was glial cells (*PLP1* and *TTHY1*), clusters D and E were neuron progenitors (*NEUROD1*), cluster F contained mitotically active neuronal cells (*FOXN4*, *PTTG1*, and *UBE2C*), and cluster G consisted of mesenchymal/muscle cells (*TAGLN* and *COL1A1*) (*SI Appendix*, Figs. S3–S5). Overall, the single-cell RNAseq data indicated that the vast majority of the culture was neuronal (∼85%) at different stages of commitment (64% fully committed neurons, 15% neuronal progenitors, and 5% mitotic neuronal progenitors). Nonneuronal cells constituted the remaining fraction of differentiated cells (13% glial and 2% mesenchymal/muscle; Fig. 4*D*). Clusters A and B were the most closely related to one another (Fig. 4*E*), sharing many highly expressed genes (*GAP43* and *NEFM*) and GO terms (growth cone and axon). Cluster B, containing the majority of the *CHX10*$^+$ cells, comprised cells expressing a number of genes consistent with an excitatory V2a interneuron phenotype, such as *SOX21*, *SHOX2*, *LHX3*, and ornithine aminotransferase (*OAT*), as well as *HOX* genes consistent with a hindbrain/cervical identity [homeobox B5 (*HOXB5*)] (*SI Appendix*, Fig. S6). Both clusters D and E were identified as early neurons (*NEUROG1*); however, cells in cluster D exhibited a more committed neuron phenotype (*RND2* and *IGDCC3*) compared with cells in cluster E (*UBE2S* and *MT2A*) (*SI Appendix*, Fig. S4). Furthermore, 80% of cells expressing the p2 marker *FOXN4* were contained within the mitotically active cluster F (*SI Appendix*, Fig. S6). Taken together, these data suggest that the V2a differentiation cultures (at day 17) yield primarily postmitotic excitatory neurons (clusters A and B) that arise from a pool of neuronal progenitors (clusters D and E) and mitotic cells (cluster F) (Fig. 4*F*) and contain an enriched population of cells expressing markers consistent with a V2a interneuron phenotype.

Long-Term Culture Increases the Maturation Profile of V2a Interneurons. To examine the maturation of V2a interneurons, differentiated cultures were dissociated after 17 d, replated, and analyzed on days 20, 30, 40, 50, and 60 of culture (Fig. 5*A*). By day 20, CHX10$^+$ cells expressed neuronal markers β_{III} tubulin and neurofilament, and expression persisted throughout 60 d of culture (*SI Appendix*, Figs. S7 *B–K* and S8 *A* and *B*). Some neuronal nuclei (NeuN) colocalized with CHX10$^+$ cells, and NeuN expression continued through day 60 (*SI Appendix*, Fig. S7 *L–P*). Vesicular glutamate transporter 2 (VGlut2), a marker of glutamatergic neurons, was not detected early (day 20; *SI Appendix*, Fig. S7*Q*), but was abundant in later-stage cultures (day 60), indicating the adoption of a mature glutamatergic fate (*SI Appendix*, Fig. S7*Y*). Although many CHX10$^+$ nuclei were readily apparent initially (day 20; *SI Appendix*, Fig. S7*B*), identification of CHX10$^+$ cells declined over time owing to reduced expression, as well as to an increase in the total number of cells in the cultures (*SI Appendix*, Fig. S8 *C* and *D*). Overall, the temporal phenotypic expression patterns support the progressive, albeit limited, maturation in vitro of the V2a interneuron cultures.

Calcium imaging was used to detect spontaneous electrical activity during extended culture as a functional indication of neuronal maturation. At different time points, individual soma of cells loaded with Fluo4 were visually identified (white arrows;

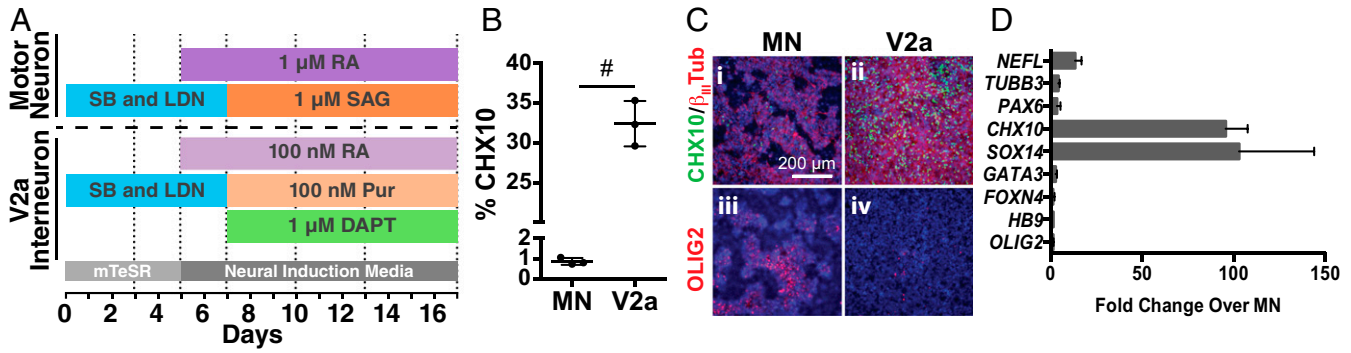

Fig. 3. V2a interneuron protocol specifically increases V2a interneuron population. (*A*) Timeline contrasting the motor neuron and V2a interneuron differentiation protocols. (*B*) Flow cytometry analysis of CHX10 for motor neuron and V2a interneuron differentiation. CHX10 expression using the V2a interneuron differentiation was greater ($P < 0.005$, by unpaired *t* test) than motor neuron differentiation. $n = 3$. (*C*) Immunostaining for CHX10 (green) and nuclei (blue). (*i* and *ii*) Immunostaining for β_{III} tubulin (red) in cultures differentiated with the motor neuron protocol (*i*) and V2a interneuron protocol (*ii*). (*iii* and *iv*) Immunostaining for OLIG2 (red) in cultures differentiated with the motor neuron protocol (*iii*) and V2a interneuron protocol (*iv*). (Scale bars: 200 μm.) (*D*) Gene expression of day 17 V2a interneuron cultures compared with day 17 motor neuron cultures. $n = 3$. Data represent mean ± SD.

SI Appendix, Fig. S9 *A* and *B*). The average change in calcium transients was measured over time. Although calcium spikes were not observed initially (day 20), they were seen more often in older cultures (day 40), with increasing amplitude and frequency (*SI Appendix*, Fig. S9*C*). Whole-cell patch-clamp recordings of individual cells were used to assess electrophysiological properties of the differentiation over time. Although the resting membrane potential did not significantly change throughout the duration of culture (~−40 mV) (*SI Appendix*, Fig. S9*D*), the action potential frequency of V2a cultures increased over time in response to current stimulation (20 pA, 1.5 s; *SI Appendix*, Fig. S9*E*, *ii*). Consistent with the observed phenotypic expression patterns, the electrophysiological properties of the differentiated cells suggest some maturation of V2a interneuron cultures over time.

Transplanted hPSC-Derived V2a Interneurons Survive and Mature in the Adult Murine Spinal Cord. The physiological response of hPSC-derived V2a interneurons within the environment of the spinal cord was examined by transplanting differentiated cultures into naïve spinal cords of C57/SCID mice. V2a interneuron cultures (~45% $CHX10^+$ cells; *SI Appendix*, Fig. S10 *A* and *B*) were transplanted at thoracic vertebral level 9 (T9), and spinal cords were harvested 2 wk later for histological analysis (*SI Appendix*, Fig. S10*C*). Transplanted cells were identified in sagittal sections with antibodies for a human cytoplasmic protein (Stem121; Fig. 5*A*) and human nuclear antigen (HNA; Fig. 5*B*). HNA^+ nuclei remained predominantly at the transplantation site, with limited migration along the rostral/caudal axis of the spinal cord. $Stem121^+$ cells were observed at the transplantation site (Fig. 5*C*), with processes extending over 5 mm in both rostral and caudal directions (Fig. 5*D*).

To assess the phenotype of the transplanted cells, adult murine spinal cord was examined by histological staining with a panel of different neuronal markers. Most of the HNA^+ cells coexpressed CHX10 (61.1% ± 10.8%), confirming the survival of transplanted V2a interneurons for at least 2 wk (Fig. 5 *E*–*G*). The vast majority of $CHX10^+$ cells expressed NeuN (91.1% ± 4.6%; Fig. 5*H*, arrows and *Inset*), and many expressed VGlut2 (Fig. 5*I*, *Inset*), indicating maturation of V2a interneurons into a glutamatergic phenotype within the spinal cord environment. Occasional $GABA^+$ cells were found in the vicinity of the transplantation site, but, as expected, $CHX10^+/GABA^+$ cells were

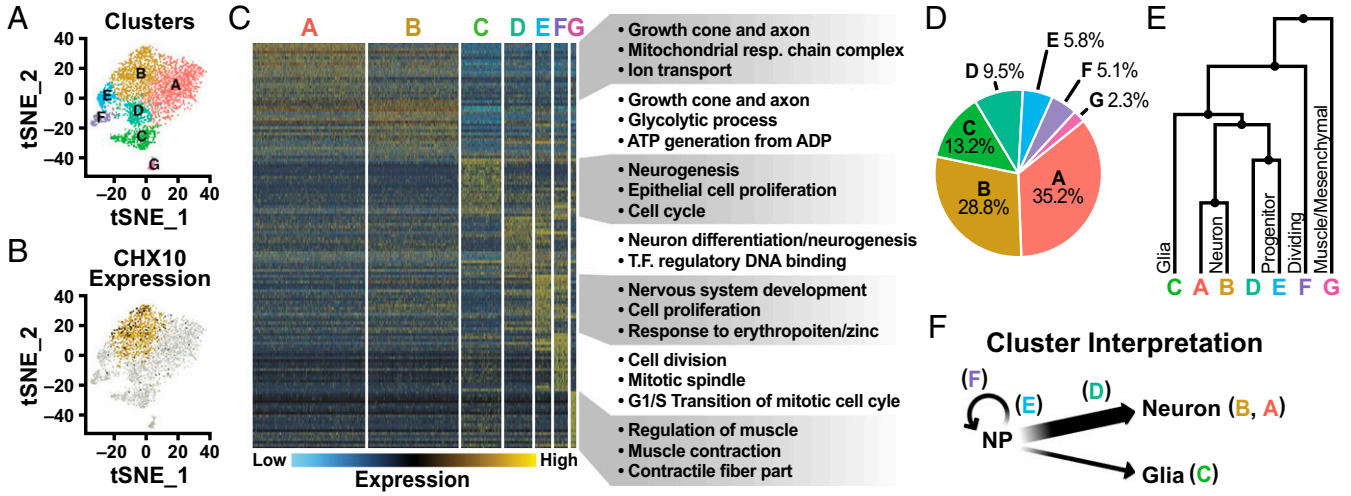

Fig. 4. Single-cell RNAseq of V2a interneuron cultures. (*A*) tSNE plot of V2a interneuron cultures indicating seven clusters. (*B*) *CHX10* expression (black dots) overlaid on cluster B (gold dots). Open circles represent the rest of the population. (*C*) Heatmap of the top 20 globally differentially expressed genes for each cluster. Expression values are normalized for each individual gene, with blue indicating low expression and yellow indicating high expression. GO terms for each cluster were determined through global and pairwise comparisons. (*D*) Percentage of cells found in each cluster. (*E*) Dendrogram of the relationships between clusters. (*F*) Interpretation of the different cell types comprising V2a interneuron cultures based on cluster analysis.

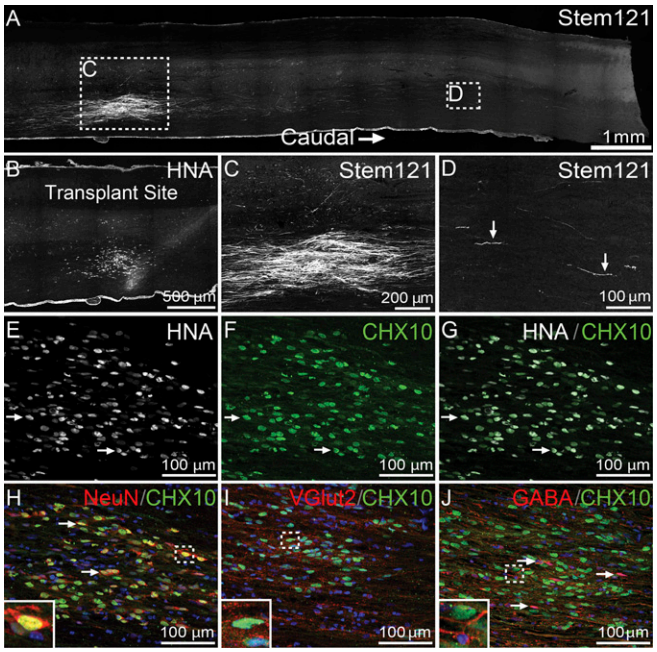

Fig. 5. hPSC-derived V2a interneurons survive and mature in the adult murine spinal cord. (*A*) Stem 121 (white) immunostaining in a sagittal tissue section caudal to T9. (*B*) HNA (white) immunostaining near the transplantation site. (*C* and *D*) Stem121 (white) immunostaining at the transplantation site (*C*) and at 5 mm from the center of the transplantation site (*D*). (*E*–*G*) HNA (white) and CHX10 (green) immunostaining of V2a interneurons at the transplantation site. (*H*–*J*) CHX10 (green) immunostaining and nuclei labeling (blue) of transplanted V2a interneurons. (*Insets*) Higher-magnification views. (*H*) NeuN (red) and inset of a $NeuN^+/CHX10^+$ nuclei. (*I*) VGlut2 (red) and inset of VGlut2 labeling adjacent to the $CHX10^+$ nuclei of a transplanted V2a interneuron. (*J*) GABA (red) and inset of a $GABA^+/CHX10^-$ cell adjacent to a $GABA^-/CHX10^+$ cell.

never detected (Fig. 5*J* and *Inset*). In addition, no $OCT4^+$ cells or signs of potential teratoma formation were observed in any of the histological sections examined (*SI Appendix*, Fig. S11 *A*–*D*).

Transplanted hPSC-derived V2a interneurons projected to multiple locations in the murine spinal cord (*SI Appendix*, Fig. S12*A*). $Stem121^+$ processes projected within the white matter, and many branched into the adjacent gray matter as well (*SI Appendix*, Fig. S12*A*, *i*). Transplanted neurons also projected axons between distinct transplantation sites (*SI Appendix*, Fig. S12*A*, *ii*). Putative synapse formations of the transplanted cell population with host cells were observed adjacent to the transplantation sites (*SI Appendix*, Fig. S12*A*, *iii*). The postsynaptic marker HOMER was found on host neurons ($NeuN^+$) in direct proximity to abutting human cell neurites ($Stem121^+$), suggesting synapse formation of transplanted cells with the host tissue (*SI Appendix*, Fig. S12 *B*–*E*). In addition, human cell neurite endings expressing the presynaptic marker synaptophysin were observed directly adjacent to host neurons (*SI Appendix*, Fig. S12 *F*–*I*). $Stem121^+$ cells also expressed the postsynaptic marker GRIP1 (*SI Appendix*, Fig. S12 *J*–*M*). These results demonstrate that transplanted hPSC-derived V2a interneurons integrate with the host tissue of the adult murine spinal cord.

Discussion

This study describes a successful differentiation of excitatory V2a interneurons from hPSCs using developmental signaling morphogens (RA and Shh agonists) to specify p2 progenitors in combination with Notch inhibition to direct V2a commitment. Initially, we tested a combination of RA, pur, and DAPT concentrations, similar to those used to promote V2a differentiation of murine ESCs (25) but applied over a comparable time scale for hPSC motor neuron differentiation (11). Compared with motor neuron differentiation, lower concentrations of RA (100 nM vs. 1 μM) increased the relative percentage of $CHX10^+$ cells (Fig. 1 *C*–*E*). In addition to the well-known caudalizing effects of RA on hindbrain and spinal neuron populations (20, 28), dorsoventral RA signaling gradients also can impact progenitor domain specification during development (20, 29, 30). In addition, a reduced concentration of Shh agonist (100 nM), compared with that required for motor neuron differentiation (1 μM), increased the relative percentage of $CHX10^+$ cells derived from hPSCs, analogous to dorsoventral patterning of the developing neural tube. Consistent with previous reports of PSC-directed differentiation to neural lineages (8, 31), V2a fate specification is sensitive to subtle in vitro changes in concentrations of the signaling molecules that pattern the neural tube. The observed variability in the yield of $CHX10^+$ cells between experiments and different cell lines (*SI Appendix*, Fig. S2*B*) could been related to a number of technical reasons that commonly afflict hPSC differentiation efficiency, such as genomic differences between cell lines, variable upstream isolation/derivation/culture methods before differentiation studies, lack of synchrony among hPSCs at the start of differentiation, and variable concentrations of endogenously produced factors.

Although coincident RA and Shh signaling pathways pattern progenitor domains in the developing neural tube, inhibition of Notch signaling is critical to the specification of V2a interneurons (Fig. 1*G*). The effects of Notch inhibition on hPSC V2a interneuron differentiation are likely two-pronged: increased hPSC neurogenesis (β_{III} $tubulin^+$) and promotion of V2a interneuron ($CHX10^+$ and $SOX14^+$) specification instead of V2b ($GATA3^+$). Notch inhibition of PSCs undergoing neural differentiation generally enhances neurogenesis (32, 33). In our study, the proportion of neuronal cells was increased by inhibiting Notch in the V2a interneuron cultures compared with the motor neuron cultures that lacked DAPT treatment (Fig. 3 *C*, *i* and *ii* and *D*). Notch signaling also regulates the balance between V2 committed cell types emanating from the p2 progenitor domain (24, 34). Expression of the V2b marker *GATA3* was low (a less than twofold increase over hPSCs) when Notch signaling was inhibited with DAPT (Fig. 2*C*), and expression of V2a transcription factors *CHX10* and *SOX14* was increased by ∼100-fold compared with motor neuron cultures that lacked Notch inhibition (Fig. 3*D*). Thus, inhibition of Notch signaling is critical to the specification of human V2a interneurons from hPSCs and exerts a compounded effect by increasing the neuronal pool along with specifying V2a interneurons from the p2 domain.

Single-cell RNAseq analysis enabled a comprehensive analysis of the cell population at day 17 of the V2a interneuron differentiation. *K*-means clustering of 12 principal components revealed that $CHX10^+$ cells were contained largely within a single cluster (cluster B; Fig. 4 *A* and *B*) that was enriched with cells of an excitatory neuronal phenotype and hindbrain/cervical identity, based on coincident expression of several genes (*OAT*, *PCP4*, and *HOXB5*). The majority of differentiated cells appeared to be committed to a neuronal fate, with distinct subpopulations (clusters A, B, D, E, and F) differing largely on the basis of stage of differentiation or activity (i.e., metabolic, mitotic) (Fig. 4 *E* and *F*), thus providing a snapshot of a dynamic differentiation process. It is not surprising that a small population of glial cells (cluster C) was detected along with a few nonneural cells (mesenchymal/muscle) when starting from PSCs, and glial cells can provide necessary support of neurons and promote maturation (35). Overall, our single-cell transcriptome results largely agreed with bulk gene analysis (Fig. 2) and confirmed the effective differentiation of excitatory neurons with phenotypic properties of V2a interneurons.

Maturation of hPSC-derived V2a interneurons is important to their physiological function and potential efficacy as a therapeutic cell type. However, a major challenge to the entire field of stem cell research is the relatively immature phenotype of most hPSC-derived cells, especially in vitro (36). Assessing V2a interneuron maturation over time was difficult in heterogeneous cultures owing to decreased expression of CHX10 and dilution by other neuronal and nonneuronal cell types (*SI Appendix*, Figs. S7 and S8). Electrophysiological analysis revealed that neurons

in V2a cultures exhibited nascent signs of maturation over time, based on increased action potential frequency in response to current injection (*SI Appendix*, Fig. S9*E*, *ii*). Prospective studies of single cells or highly enriched populations of $CHX10^+$ cells are needed to rigorously define the phenotypic markers and electrophysiological properties of human V2a interneurons.

To examine survival and maturation within the native CNS environment, hPSC-derived V2a interneurons were transplanted into the adult murine spinal cord. Transplanted human cells in the spinal cord exhibited limited migration, with the majority of HNA^+ and $Stem121^+$ cells found within 1 mm of the transplantation site. However, numerous $Stem121^+$ processes resembling axons projected out from the sites of transplantation and were identified at least 5 mm away, similar to endogenous murine V2a interneurons that can extend over four spinal segments (>2.5 mm) in the rostral and caudal directions (37). Although transplanted $CHX10^+$ human V2a interneurons matured into glutamatergic neurons expressing NeuN and VGlut2, whether human V2a interneurons adopt an appropriate laminar location and rostral/caudal phenotype depending on the site of transplantation remains to be clarified. Functional integration of transplanted V2a interneuron cultures within spinal cord tissue was suggested by the expression of presynaptic (synaptophysin) and postsynaptic (HOMER and GRIP1) markers at the interface of transplanted cell neurites and host neurons (*SI Appendix*, Fig. S10 *E–M*). In future studies, it will be necessary to functionally assess the electrical connectivity of human V2a interneurons with endogenous spinal neurons to determine whether proper synapses with motor circuits are formed. The lack of teratoma formation and absence of $Oct4^+$ cells in histological sections indicated that nonpurified, but highly enriched, V2a interneuron cultures were safe for transplantation. Overall, these data demonstrate that hPSC-derived V2a interneurons survive, adopt a glutamatergic phenotype, extend long-distance axons, and form putative synapses with host neurons when transplanted into the adult murine spinal cord.

In conclusion, this report provides a description of V2a interneurons differentiated from hPSCs through manipulation of RA, Shh, and Notch signaling pathways. These cells provide insight into the phenotypic properties of human V2a interneurons and represent a potent new candidate for regenerative cell therapies to treat CNS injuries and restore motor function.

Methods

All work with human ESC and iPSC lines was approved by the University of California – San Francisco Human Gamete, Embryo and Stem Cell Research (GESCR) Committee. All human PSC lines were grown to 70% confluence and passaged as single cells every 3 d. Dissociated cells were replated on Matrigel-coated cultureware at a density of 10,000 cells per cm^2 with 10 μM ROCK inhibitor in mTeSR. The experimental procedures, including V2a interneuron differentiation, neuronal maturation, endpoint analysis, imaging analysis and quantification, electrophysiology testing, single-cell RNAseq, spinal transplantation, and statistical analysis, are described in detail in *SI Appendix, Methods*.

ACKNOWLEDGMENTS. We thank the following individuals for helpful discussions and assistance with manuscript preparation: Dr. Shelly Sakiyama-Elbert, Dr. Biljana Djukic, Alex Williams and staff the Gladstone Bioinformatics Core, Meredith Calvert and staff at the Gladstone Histology and Light Microscopy Core, staff at the Gladstone Stem Cell Core, Oriane Matthys, Dr. Nathaniel Huebsch, Giovanni Maki, and David Joy. We also thank Dr. Bruce Conklin for generously providing the WTB and WTC hiPSC cell lines and Dr. Thomas Fandel for guidance and assistance in cell transplantation. This work was supported by California Institute of Regenerative Medicine Grant LA1-08015 (to T.C.M.) and the Alvera Kan Endowed Chair (L.N.-H.). J.C.B. was supported by a National Science Foundation (NSF) Graduate Research Fellowship and previously by an NSF Stem Cell Biomanufacturing Integrative Graduate Education and Research Traineeship (DGE 0965945). C.A.G. is a Howard Hughes Medical Institute Fellow of the Damon Runyon Cancer Research Foundation (DRG-2206-14).

1. Keirstead HS, et al. (2005) Human embryonic stem cell-derived oligodendrocyte progenitor cell transplants remyelinate and restore locomotion after spinal cord injury. *J Neurosci* 25:4694–4705.
2. Guest J, Santamaria AJ, Benavides FD (2013) Clinical translation of autologous Schwann cell transplantation for the treatment of spinal cord injury. *Curr Opin Organ Transplant* 18:682–689.
3. Cummings BJ, et al. (2005) Human neural stem cells differentiate and promote locomotor recovery in spinal cord-injured mice. *Proc Natl Acad Sci USA* 102:14069–14074.
4. Cizkova D, et al. (2007) Functional recovery in rats with ischemic paraplegia after spinal grafting of human spinal stem cells. *Neuroscience* 147:546–560.
5. Lu P, et al. (2012) Long-distance growth and connectivity of neural stem cells after severe spinal cord injury. *Cell* 150:1264–1273.
6. Shi Y, Kirwan P, Livesey FJ (2012) Directed differentiation of human pluripotent stem cells to cerebral cortex neurons and neural networks. *Nat Protoc* 7:1836–1846.
7. Perrier AL, et al. (2004) Derivation of midbrain dopamine neurons from human embryonic stem cells. *Proc Natl Acad Sci USA* 101:12543–12548.
8. Maroof AM, et al. (2013) Directed differentiation and functional maturation of cortical interneurons from human embryonic stem cells. *Cell Stem Cell* 12:559–572.
9. Nicholas CR, et al. (2013) Functional maturation of hPSC-derived forebrain interneurons requires an extended timeline and mimics human neural development. *Cell Stem Cell* 12:573–586.
10. Li XJ, et al. (2005) Specification of motoneurons from human embryonic stem cells. *Nat Biotechnol* 23:215–221.
11. Amoroso MW, et al. (2013) Accelerated high-yield generation of limb-innervating motor neurons from human stem cells. *J Neurosci* 33:574–586.
12. Butt SJ, Harris-Warrick RM, Kiehn O (2002) Firing properties of identified interneuron populations in the mammalian hindlimb central pattern generator. *J Neurosci* 22:9961–9971.
13. Butt SJ, Kiehn O (2003) Functional identification of interneurons responsible for left-right coordination of hindlimbs in mammals. *Neuron* 38:953–963.
14. Ericson J, et al. (1997) Pax6 controls progenitor cell identity and neuronal fate in response to graded Shh signaling. *Cell* 90:169–180.
15. Azim E, Jiang J, Alstermark B, Jessell TM (2014) Skilled reaching relies on a V2a propriospinal internal copy circuit. *Nature* 508:357–363.
16. Zhong G, et al. (2010) Electrophysiological characterization of V2a interneurons and their locomotor-related activity in the neonatal mouse spinal cord. *J Neurosci* 30:170–182.
17. Crone SA, et al. (2008) Genetic ablation of V2a ipsilateral interneurons disrupts left-right locomotor coordination in mammalian spinal cord. *Neuron* 60:70–83.
18. Crone SA, et al. (2012) Irregular breathing in mice following genetic ablation of V2a neurons. *J Neurosci* 32:7895–7906.
19. Al-Mosawie A, Wilson JM, Brownstone RM (2007) Heterogeneity of V2-derived interneurons in the adult mouse spinal cord. *Eur J Neurosci* 26:3003–3015.
20. Okada Y, Shimazaki T, Sobue G, Okano H (2004) Retinoic acid concentration-dependent acquisition of neural cell identity during in vitro differentiation of mouse embryonic stem cells. *Dev Biol* 275:124–142.
21. Marklund U, et al. (2014) Detailed expression analysis of regulatory genes in the early developing human neural tube. *Stem Cells Dev* 23:5–15.
22. Karunaratne A, Hargrave M, Poh A, Yamada T (2002) GATA proteins identify a novel ventral interneuron subclass in the developing chick spinal cord. *Dev Biol* 249:30–43.
23. Li S, Misra K, Matise MP, Xiang M (2005) Foxn4 acts synergistically with Mash1 to specify subtype identity of V2 interneurons in the spinal cord. *Proc Natl Acad Sci USA* 102:10688–10693.
24. Del Barrio MG, et al. (2007) A regulatory network involving Foxn4, Mash1, and delta-like 4/Notch1 generates V2a and V2b spinal interneurons from a common progenitor pool. *Development* 134:3427–3436.
25. Brown CR, Butts JC, McCreedy DA, Sakiyama-Elbert SE (2014) Generation of v2a interneurons from mouse embryonic stem cells. *Stem Cells Dev* 23:1765–1776.
26. Iyer NR, Huettner JE, Butts JC, Brown CR, Sakiyama-Elbert SE (2016) Generation of highly enriched V2a interneurons from mouse embryonic stem cells. *Exp Neurol* 277:305–316.
27. Lian X, et al. (2013) Directed cardiomyocyte differentiation from human pluripotent stem cells by modulating Wnt/β-catenin signaling under fully defined conditions. *Nat Protoc* 8:162–175.
28. Kessel M (1992) Respecification of vertebral identities by retinoic acid. *Development* 115:487–501.
29. Pierani A, Brenner-Morton S, Chiang C, Jessell TM (1999) A sonic hedgehog-independent, retinoid-activated pathway of neurogenesis in the ventral spinal cord. *Cell* 97:903–915.
30. Wilson L, Gale E, Chambers D, Maden M (2004) Retinoic acid and the control of dorsoventral patterning in the avian spinal cord. *Dev Biol* 269:433–446.
31. Wichterle H, Lieberam I, Porter JA, Jessell TM (2002) Directed differentiation of embryonic stem cells into motor neurons. *Cell* 110:385–397.
32. Borghese L, et al. (2010) Inhibition of notch signaling in human embryonic stem cell-derived neural stem cells delays G1/S phase transition and accelerates neuronal differentiation in vitro and in vivo. *Stem Cells* 28:955–964.
33. Crawford TQ, Roelink H (2007) The notch response inhibitor DAPT enhances neuronal differentiation in embryonic stem cell-derived embryoid bodies independently of sonic hedgehog signaling. *Dev Dyn* 236:886–892.
34. Skaggs K, Martin DM, Novitch BG (2011) Regulation of spinal interneuron development by the Olig-related protein Bhlhb5 and Notch signaling. *Development* 138:3199–3211.
35. Müller HW, Seifert W (1982) A neurotrophic factor (NTF) released from primary glial cultures supports survival and fiber outgrowth of cultured hippocampal neurons. *J Neurosci Res* 8:195–204.
36. Cornacchia D, Studer L (2017) Back and forth in time: Directing age in iPSC-derived lineages. *Brain Res* 1656:14–26.
37. Dougherty KJ, Kiehn O (2010) Firing and cellular properties of V2a interneurons in the rodent spinal cord. *J Neurosci* 30:24–37.